gene (Firth & Atkins, 2009). There are reports that NS1′ plays an important role in the increased virulence of WNV and JEV (Melian *et al.*, 2010; Ye *et al.*, 2012). A recent report showed that NS1′ co-localizes with NS1 and substitutes for NS1 in WNV replication (Young *et al.*, 2013). Flaviviruses expressing NS1′ have been suggested to have been evolutionarily selected for an advantage in virus replication/transmission in the mosquito–host cycle (Melian *et al.*, 2010).

The present study focused on the JEV NS1′ protein and on the elucidation of its molecular function(s), especially in avian cells. Our study showed that a mutation at nt 67 in the NS2A-coding region of JEV was critical for NS1′ production. We have revealed that the NS1′ protein facilitated JEV production in avian cells based on the increasing viral RNA level. This protein was found to co-localize efficiently with cytoplasmic NS5 protein (an RNA-dependent RNA polymerase) in avian cells. *In vivo*, NS1′ expression enhanced virus production and increased mortality in embryonated chicken eggs (ECEs). These results suggest a novel fundamental role of the NS1′ protein in avian cells by influencing efficient survival of JEV in the natural transmission cycle through the facilitation of virus production in these cells.

RESULTS

NS2A G67A mutation abolishes NS1′ protein production

Two JEV infectious clones (ICs), S982-IC and JaTH-IC, used in this study differed in expressing NS1′ in mammalian (BHK) and avian (DF-1) cells. S982-IC did not express NS1′ in these vertebrate cells but expressed NS1 protein, whereas JaTH-IC expressed both NS1′ and NS1 proteins in these cells (Fig. 1a). In S982-IC, an A was present at nt 67 of the *NS2A* gene, whereas JaTH-IC had a G in this position instead (Figs 1b and S1a, available in JGV Online). Analysis of the RNA secondary structure of this gene predicted that this nucleotide change disrupted the pseudoknot structure, which was critical for the −1 ribosomal frameshifting (Fig. S1b). A point mutation was introduced at nt 67 in the *NS2A* gene of the two clones as described in Methods, and the constructed ICs were designated S982-A67G-IC, which was able to produce NS1 and NS1′ proteins, and JaTH-G67A-IC, which produced NS1 but not NS1′ proteins as expected (Fig. 1c). These results indicated that the G at position 67 in NS2A coding region plays a critical role in production of the NS1′ protein. The G67A mutation resulted in a V23I amino acid mutation in the NS2A protein. In order to eliminate the influence of the amino acid change from I to V at position 23 of NS2A, JaTH-G66A-IC was developed. JaTH-G66A-IC produced NS1 but not NS1′ proteins as expected (Fig. 1c). A description of the original ICs and mutated clones with respect to nucleotide and amino acid differences and NS1′ expression is given in Table S1.

Expression levels of NS1′ protein in DF-1 and BHK cells

NS1′ expression by JEV ICs in avian cells (DF-1) was compared with that in mammalian cells (BHK) at 48 h post-infection (p.i.). The bands for the NS1′ protein showed a four- to fivefold greater intensity compared with those of the NS1 protein in the DF-1 cells infected with NS1′-expressing viruses (S982-A67G-IC and JaTH-IC). In contrast, bands of similar intensity were observed for the NS1′ and NS1 proteins in BHK cells infected with the same viruses (Fig. 1c).

NS1′ protein expression facilitates virus production in avian cells

Some noteworthy findings arose after comparing the growth characteristics of the ICs in BHK and DF-1 cells (Fig. 2). Foci of similar size were formed in BHK cells that were infected with any of the ICs (Fig. 2a); however, larger foci were formed in avian DF-1 cells when infected with the NS1′-expressing viruses (Fig. 2b).

Growth curves showed that the titres of the NS1′-expressing viruses were over 10 times higher than those of the NS1′-non-expressing viruses (S982-IC, JaTH-G67A-IC and JaTH-G66A-IC) at 48 and 72 h p.i. in DF-1 cells (Fig. 2c); however, all of the ICs showed almost equal titres in BHK cells. These results indicated that NS1′ expression can enhance virus propagation in avian cells.

NS1′ protein co-localizes with NS5 protein

NS1′-specific polyclonal antibodies were produced as described in Methods. These antibodies were found to detect only NS1′ in cells infected with the NS1′-expressing viruses by Western blotting and immunofluorescent staining (Fig. 3a, b). In contrast, the anti-NS1 antibodies could not discriminate between the NS1 and NS1′ proteins (Fig. 3b). With the application of anti-NS1′ antibodies and anti-NS5 antibodies, NS1′ proteins were found to co-localize with NS5 proteins in BHK and DF-1 cells that were infected with the NS1′-expressing viruses (Fig. 4). This co-localization was observed at 12 h p.i. and increased over time (data not shown).

NS1′ protein efficiently interacts with NS5 protein in avian cells

A higher co-localization rate of NS1′ and NS5 in DF-1 cells was noted by confocal laser-scanning microscopy analysis. A 20–30 % co-localization of NS1′ and NS5 was observed in BHK cells infected with the NS1′-expressing viruses, whereas 60–70 % was observed in DF-1 cells infected with the same viruses (Fig. 4).

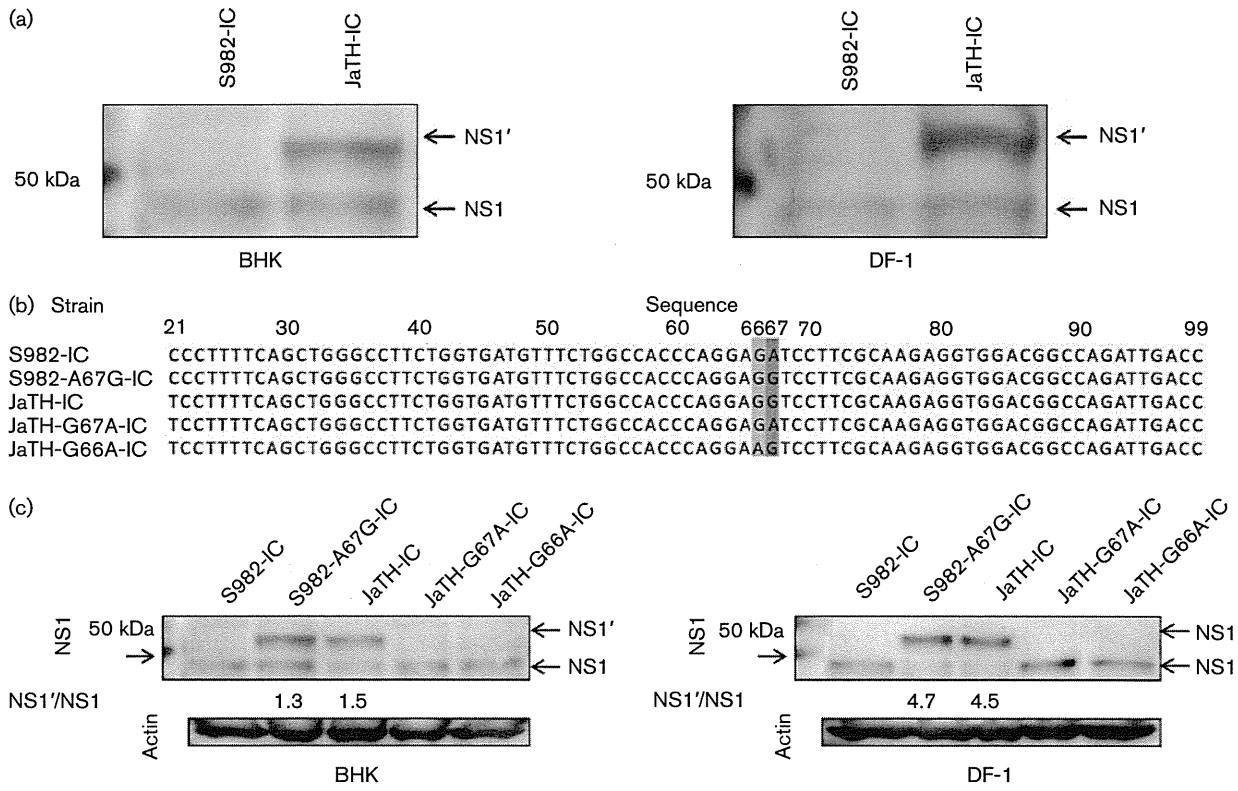

Fig. 1. NS1′ expression and alignment of nucleotide sequences of the studied viruses. (a) Detection of NS1 and NS1′ in JEV-infected cells. BHK and DF-1 cells were infected at an m.o.i. of 10 for 48 h with S982-IC or JaTH-IC. Cellular extracts were subjected to Western blotting with JEV anti-NS1 polyclonal antibodies. (b) Alignment of nucleotide sequences in the NS2A gene of the five viruses used in this study. The number above the sequence indicates nucleotide position in the NS2A gene. The nucleotides at positions 66 and 67 of the NS2A gene are highlighted in light grey and dark grey, respectively. Alignment of the NS2A gene showed that JaTH-G66A-IC had an A at position 66, and S982-IC and JaTH-G67A-IC had an A at position 67 of NS2A gene. (c) Detection of NS1 and NS1′ in BHK and DF-1 cells infected with the indicated viruses at an m.o.i. of 10 for 48 h. Cellular extracts were subjected to Western blotting for the detection of proteins indicated on the left side of the figure, with β-Actin as the internal control. The number below a band lane indicates relative intensity of NS1′ band divided by the intensity of NS1 band.

Co-immunoprecipitation (Co-IP) by purified anti-NS1 or anti-NS5 antibodies resulted in the co-precipitation of NS5 and NS1/NS1′ in the lysates of BHK and DF-1 cells infected with JEV ICs (Fig. 5a, b). The NS5 protein levels in DF-1 cells infected with the NS1′-expressing viruses were 1.8–2.2 times higher in comparison with those infected with the NS1′-non-expressing viruses when they were co-precipitated by the anti-NS1 antibodies (Fig. 5a). In contrast, in BHK cells infected with all the studied viruses, a similar amount of co-precipitated NS5 proteins was observed (Fig. 5a). A similar amount of NS1 proteins was observed in BHK and DF-1 cells when they were co-precipitated by the anti-NS5 antibodies (Fig. 5b). However, NS1′ protein levels in DF-1 cells infected with the NS1′-expressing viruses were three to four times higher in comparison with those in BHK cells that were infected with the same viruses (Fig. 5b). These results suggested that NS1′ proteins can directly or indirectly interact with NS5 proteins as well as with NS1 proteins, and that this interaction is highly efficient in avian DF-1 cells.

NS1′ protein increases viral RNA levels in avian cells

Real-time quantitative reverse transcription (RT)-PCR analysis revealed that the NS1′ protein expression significantly upregulated viral RNA copy number in DF-1 cells but not in BHK cells (Fig. 6). The viral RNA level was 10 times higher in the NS1′-expressing viruses when compared with that in the NS1′-non-expressing viruses from 12 up to 72 h p.i. in DF-1 cells (Fig. 6b). A significant difference in RNA copy number was observed between S982-IC and S982-A67G-IC at 24, 36, 48 and 72 h p.i. in DF-1 cells (Fig. 6b). A significant difference in RNA copy number was also observed between JaTH-IC and JaTH-G67A-IC at 24, 36 and 72 h p.i. in DF-1 cells. In addition, a significant difference in RNA copy number was observed between JaTH-IC and JaTH-G66A-IC at 12, 24, 36, 48 and 72 h p.i. in DF-1 cells (Fig. 6b). In contrast, RNA level was not significantly different among the studied viruses in BHK

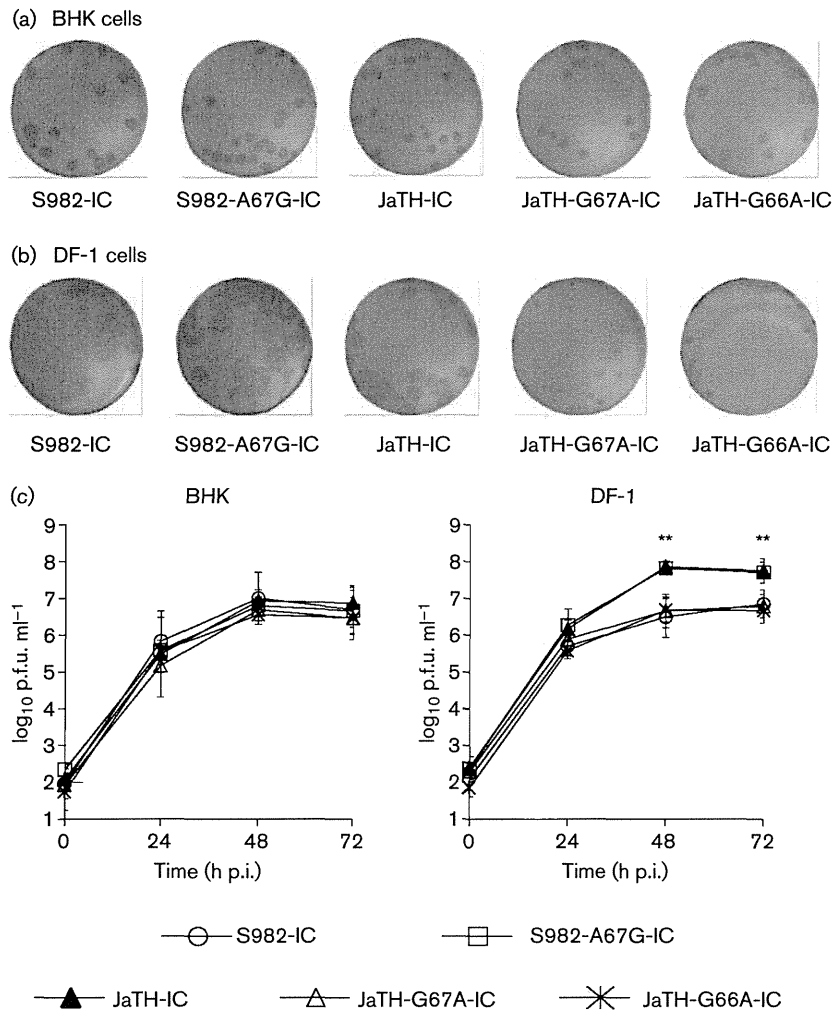

Fig. 2. Focus formation and growth curves in BHK and DF-1 cells. (a, b) BHK (a) and DF-1 (b) cells were infected with the indicated viruses, and differences in focus morphology caused by these viruses were compared on day 3 p.i. (c) Titres of virus from the supernatants of cells infected with the ICs (m.o.i. 0.1) were measured at the indicated times p.i. The values among groups were tested by one-way ANOVA analysis. Statistically significant differences in titres between the NS1′-expressing viruses (S982-A67G-IC and JaTH-IC) and the NS1′-non-expressing viruses (S982-IC, JaTH-G67A-IC and JaTH-G66A-IC) are indicated (**$P<0.01$). Results are expressed as means ± SD from three independent experiments.

cells (Fig. 6a). It was concluded that NS1′ protein expression enhanced viral RNA level only in avian cells.

NS1′ protein increases virus production and mortality in ECEs

There are some studies on the use of ECEs as a flavivirus infection model (Crespo *et al.*, 2009; Osorio *et al.*, 2012). Survival curves of ECEs infected with the NS1′-expressing and NS1′-non-expressing viruses were compared to reveal the influence of NS1′ expression. The survival curves showed that the NS1′-expressing viruses at a dose of both 10^4 and 10^2 p.f.u. per egg killed all ECEs by 6–9 days post-inoculation (Fig. 7a, b). In contrast, infection of ECEs with the NS1′-non-expressing viruses at a dose of 10^4 and 10^2 p.f.u. per egg resulted in a mortality of 80–100 % (S982-IC, 100 %; JaTH-G67A-IC, 80 %; JaTH-G66A-IC, 80 %; Fig. 7a) and 40–70 % (S982-IC, 70 %; JaTH-G67A-IC, 50 %; JaTH-G66A-IC, 40 %; Fig. 7b), respectively. All the viruses studied in this paper showed 100 % mortality in ECEs after inoculation of 10^5 p.f.u. per egg (data not shown).

On day 5 after inoculation of 10^4 p.f.u. per egg, embryonic tissues and yolk sac tissues from live and dead ECEs were collected and the recovered virus titres were compared. A significant increase in virus titre was observed in both embryonic and yolk sac tissues infected with the NS1′-expressing viruses (Fig. 7c, d). No significant difference in virus amount was observed in the tissues taken from live ECEs and from the dead ECEs infected with the same virus for both the NS1′-expressing and NS1′-non-expressing viruses. In 7-day-old ECEs, it was difficult to distinguish each organ, and no significant difference in virus amount was observed between embryo tissues and yolk sac tissues in each infected ECEs (Fig. S2a). In 14-day-old ECEs, tissue tropism was compared between the NS1′-expressing virus JaTH-IC and the NS1′-non-expressing virus JaTH-G66A-IC (Fig. S2b). The titre of virus in each tissue/organ infected with the NS1′-expressing virus was relatively higher than that infected with the NS1′-non-expressing virus. A significant difference between the two viruses was observed only in the liver (Fig. S2c).

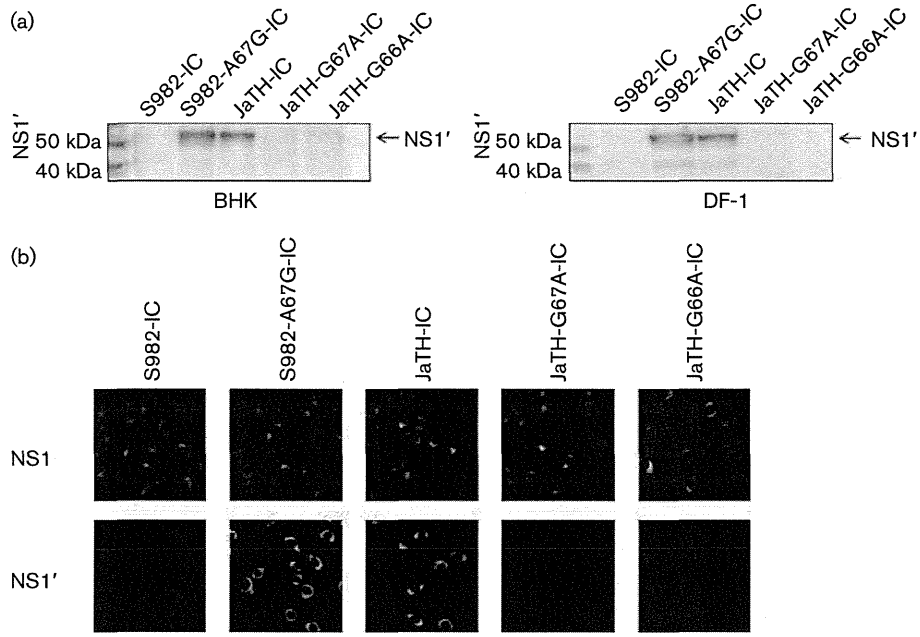

Fig. 3. Specificity of NS1′ antibodies. (a) The specificity of antibodies against NS1′ protein was confirmed by Western blotting. BHK and DF-1 cells were infected with each virus at an m.o.i. of 10. Western blotting was carried out on the extracted proteins and NS1′-specific polyclonal antibodies produced as described in Methods were used as detecting antibodies. (b) Subcellular localization of NS1 and/or NS1′ was observed in BHK cells. Anti-NS1 or anti-NS1′ antibodies were used as primary antibodies, and Alexa Fluor 568-conjugated anti-mouse antibodies were used for secondary labelling. The anti-NS1 antibodies detected NS1 and NS1′ in all five viruses, whereas the anti-NS1′ antibodies detected NS1′ only in the NS1′-expressing viruses.

DISCUSSION

Although there are a number of reports on the roles of NS1 in virus replication (Khromykh *et al.*, 1999; Lindenbach & Rice, 1997, 1999; MacKenzie *et al.*, 1996; Muylaert *et al.*, 1996; Youn *et al.*, 2012), only a few reports have dealt with the function(s) of NS1′. These reports on NS1′ have suggested that this protein has no critical effect on virus

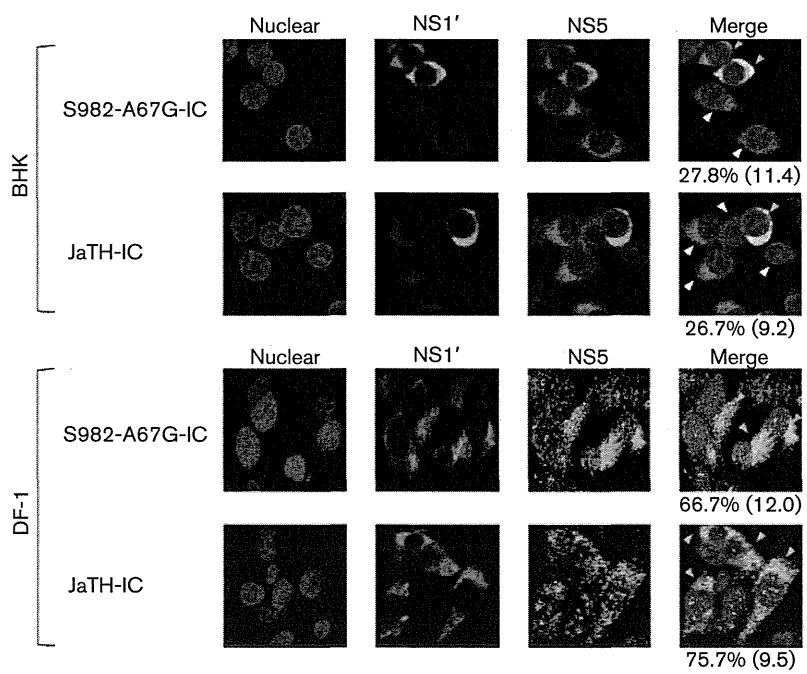

Fig. 4. Subcellular co-localization of NS1′ with NS5 in BHK and DF-1 cells. BHK and DF-1 cells were infected with the NS1′-expressing viruses (S982-A67G-IC and JaTH-IC) at an m.o.i. of 10, and the subcellular localization of NS1′ and NS5 was compared at 48 h p.i. Nuclear staining was achieved using DAPI. The number shown below the merged image indicates the co-localization percentage of NS1′ and NS5 signals. The percentage was calculated as the number of NS1′ and NS5 double-positive cells (red arrowheads) divided by the number of NS5-positive cells (white arrowheads) and is shown as the mean value from ten fields with SD indicated in parentheses.

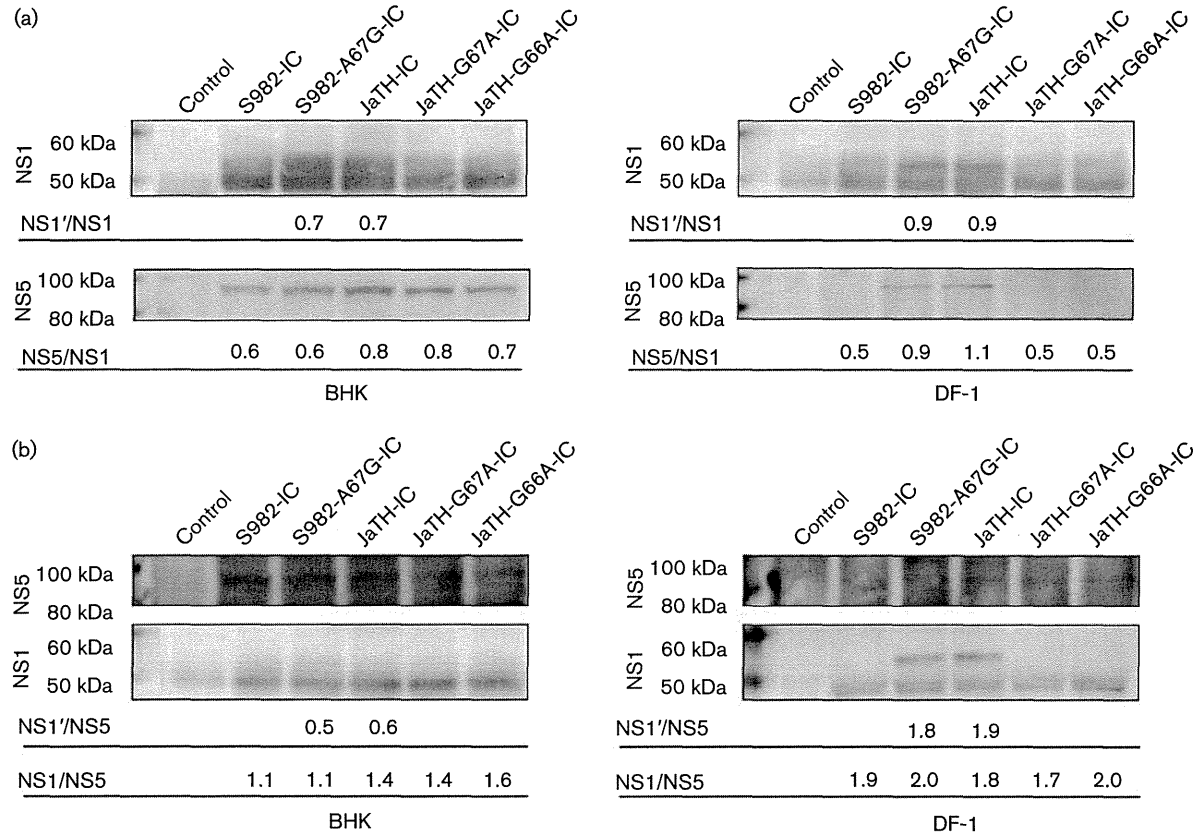

Fig. 5. Co-IP of NS1′ and NS5. (a) BHK and DF-1 cells were infected with S982-IC, S982-A67G-IC, JaTH-IC, JaTH-G67A-IC or JaTH-G66A-IC. PBS was used as a control. Co-IP was performed with purified anti-NS1 antibodies as indicated in Methods. The eluted samples were subjected to Western blotting with anti-NS1 and anti-NS5 antibodies, as indicated. (b) BHK and DF-1 cells were infected with the viruses used in (a). PBS was used as a control. Co-IP was performed with purified anti-NS5 antibodies as indicated in Methods. The eluted samples were subjected to Western blotting by anti-NS5 antibodies and anti-NS1 antibodies, as indicated. The numbers below lanes in (a) indicate the relative intensity of the NS1′ or NS5 band divided by the intensity of the NS1 band. The numbers below lanes in (b) indicate the relative intensity of the NS1 or NS1′ band divided by the intensity of the NS5 band.

propagation (Melian *et al.*, 2010; Winkelmann *et al.*, 2011; Ye *et al.*, 2012). A recent report demonstrated that NS1′ and NS1 are co-localized in viral RNA replication sites in infected cells, that NS1′ can complement for the deleted NS1 during virus replication and that there is no significant difference in the efficiency of complementation between NS1 and NS1′ (Young *et al.*, 2013). In the present report, it was demonstrated that NS1′ protein facilitated virus production based on the increasing viral RNA level in avian cells (Figs 2 and 6). An NS1′-induced increase in virus production and mortality of the ECEs was observed (Fig. 7). It was also demonstrated that NS1′ was expressed more efficiently in avian DF-1 cells (Fig. 1c) than in BHK cells, which were used in previous reports (Melian *et al.*, 2010; Winkelmann *et al.*, 2011; Ye *et al.*, 2012). NS1′ expression and growth characteristics in porcine kidney cells (PS cells) and Green monkey kidney cells (Vero cells) were similar with those in BHK cells (Fig. S3). These findings suggest that NS1′ plays a crucial role in RNA synthesis and production of JEV, especially in avian cells.

The results of this study also provide some noteworthy insights on NS1′ molecular functions. First, NS1′ expression was three to four times higher in DF-1 cells than in mammalian cells (Figs 1c and S3a). Ribosomal frameshifting is a translational mechanism used by many viruses to co-ordinately express two proteins from a single mRNA at a defined ratio (Brierley *et al.*, 2007). It has been reported that the species from which ribosomes are derived could influence the frequency of frameshifting (Matsufuji *et al.*, 1996), and a different structure of different ribosomes could influence −1 ribosomal frameshifting efficiencies (Plant & Dinman, 2006). Birds and mammals may have a different translational mechanism regarding the −1 ribosomal frameshifting, and the higher ratio of NS1′ translation could occur in avian cells. Secondly, quantitative RT-PCR analysis revealed that NS1′ increased viral

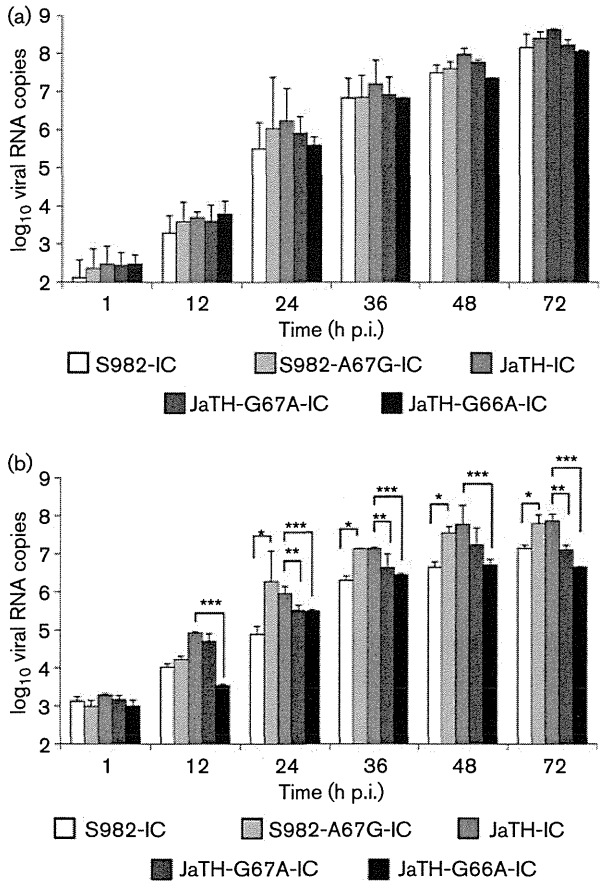

Fig. 6. Viral RNA level in BHK and DF-1 cells. Viral RNA copies from cell lysates were measured by real-time quantitative RT-PCR. (a, b) BHK (a) and DF-1 (b) cells were infected with the indicated viruses at an m.o.i. of 0.1. Viral RNA copies were measured at the indicated times p.i. The values were normalized to expression of β-actin and glyceraldehyde 3-phosphate dehydrogenase (GAPDH) for mouse and avian cells, respectively. The values between two groups were tested by Student's *t*-test or Welch test analysis. Asterisks indicate statistical significance between viruses at $P<0.05$: *, S982-IC versus S982-A67G-IC; **, JaTH-IC versus JaTH-G67A-IC; ***, JaTH-IC versus JaTH-G66A-IC. Results are expressed as means ± SD from three independent experiments.

RNA copy number in DF-1 cells but not in BHK cells (Fig. 6). A higher co-localization rate and effective interactions were also shown to occur between NS1′ and NS5 proteins in avian cells (Figs 4 and 5). These results indicate that the efficient interaction of NS1′ and NS5 may influence effective viral RNA replication in avian cells. In future studies, the role of NS1′ in replication could be elaborated further by a complementation assay (Young *et al.*, 2013). Thirdly, the NS1′-expressing viruses increased virus production and mortality rate in ECEs (Fig. 7). The present study reports for the first time the characteristic effects of JEV infection in ECEs. It will be important to reveal in future investigations how NS1′ expression affects viral pathogenicity, and the duration of a higher viraemia titre in adult birds. In JEV natural transmission, over 90 bird species are known to be amplification and reservoir hosts of JEV, and they represent the primary effective animal hosts because they can be highly viraemic and can be an outstanding source of infection for mosquitoes (Le Flohic *et al.*, 2013). Over long distances, migratory birds are the most likely spreader of JEV because some have a complex migration system over a large geographical area (van den Hurk *et al.*, 2009). Based on these situations, adaptation to birds provides a good advantage for JEV survival, and the NS1′-expressing virus showed higher fitness in avian cells (Fig. S4).

In conclusion, this study indicates that one of the intrinsic functions of the NS1′ protein found to be specific for avian cells and tissues is to facilitate virus production. The NS1′ protein works efficiently with NS5 proteins and increases viral RNA synthesis. This suggests a possible important role for NS1′ in reservoir birds by contributing to the survival of JEV through the retention of sufficient amounts of virus during the natural cycles by facilitating virus production in avian hosts.

METHODS

Cells and viruses. Baby hamster kidney (BHK) and chicken embryonic fibroblast (DF-1) cells were maintained in minimum essential medium (MEM) with 10 % FCS and 0.2 mM non-essential amino acids. BHK and DF-1 cells were allowed to grow at 37 °C with 5 % CO_2. JEV strain JaOArS982 was isolated from a *Culex* mosquito pool in Osaka, Japan, in 1982 (Sumiyoshi *et al.*, 1987). JEV strain JaTH160 was isolated from a human brain in Tokyo, Japan, in 1960 (Fujii *et al.*, 2008). Following a procedure described previously (Hayasaka *et al.*, 2004; Morita *et al.*, 2001), full-length JEV cDNA ICs designated S982-IC and JaTH-IC were constructed (Takamatsu *et al.*, unpublished data).

Mutagenesis of ICs. Site-directed mutagenesis was introduced as described previously (Yu *et al.*, 2007a) to substitute an A with a G at nt 67 of the *NS2A* gene (A67G) in the IC S982-IC, and a G with an A at nt 66 and 67 of the *NS2A* gene (G66A and G67A, respectively) in the other clone JaTH-IC. The primers used for mutagenesis are indicated in Table S2. The sequences of recovered viruses were confirmed and the resulting mutated viruses were designated S982-A67G-IC, JaTH-G67A-IC and JaTH-G66A-IC, respectively. It has been reported that the nucleotide change from G to A at nt 66 of the *NS2A* gene abolishes NS1′ expression in JEV (Ye *et al.*, 2012). In order to eliminate the influence of the amino acid change from I to V at aa 23 of the *NS2A*, JaTH-G66A-IC was developed. The experimental protocols were approved by the committee for recombinant DNA experiments, Nagasaki University, Japan (approval number: 0909021017).

Recovery of infectious virus. Full-length cDNA clones were linearized and transcribed into RNA using an SP6 transcription system as described previously (Hayasaka *et al.*, 2004), and the RNA was introduced into BHK cells by electroporation (Hayasaka *et al.*, 2004). The full-length cloned viruses were propagated in BHK cells to generate working stocks, and these virus stocks were stored at −80 °C.

Growth curves in BHK and DF-1 cells. JEV infection was performed on a monolayer of cells on 24-well plates at an m.o.i. of 0.1. After incubation for 60 min, the virus inoculum was removed and the cells were washed twice with PBS. Medium (0.5 ml) was added to each well and the plates were incubated at 37 °C under 5 %

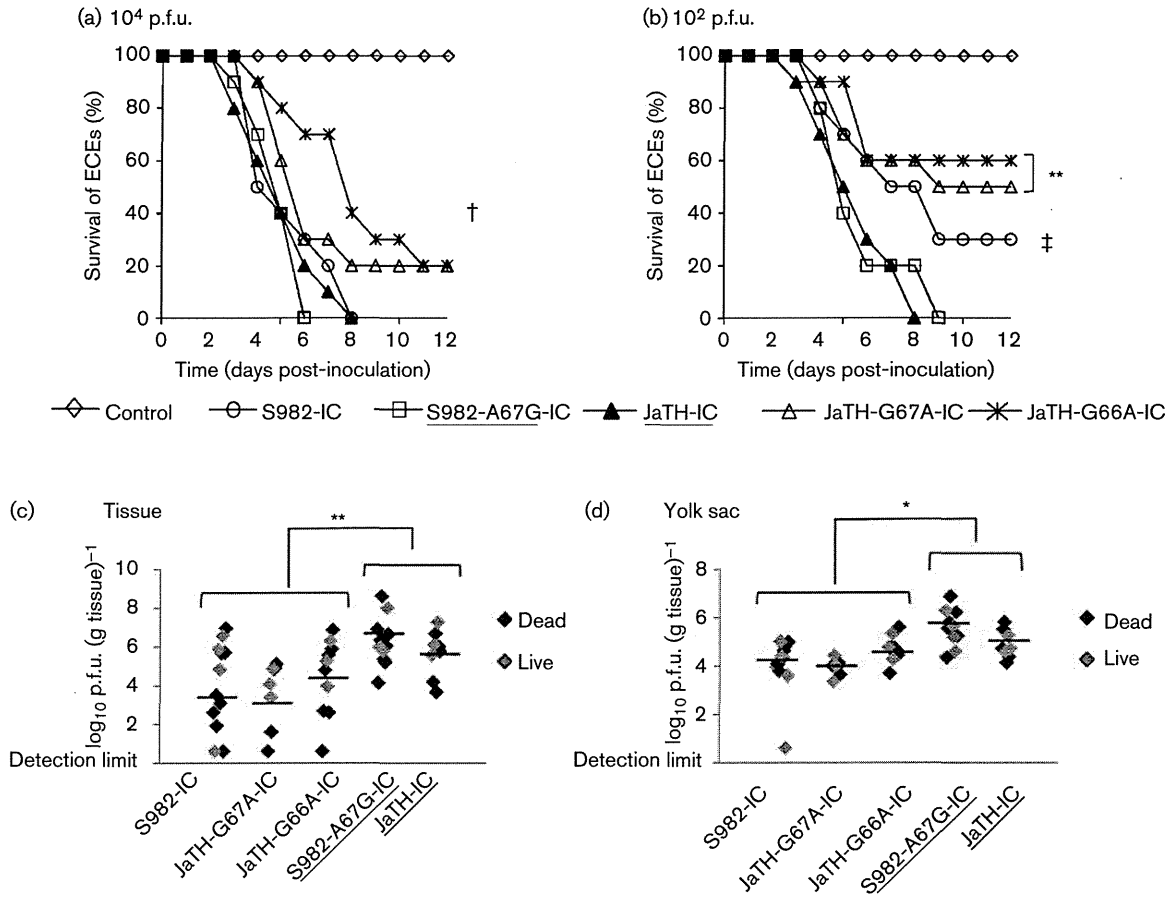

Fig. 7. Survival curves and virus titres from tissues of live and dead ECEs. (a, b) Seven-day-old ECEs (n=10) were inoculated by the indicated viruses at a titre of 10^4 p.f.u. per egg (a) or 10^2 p.f.u. per egg (b). Survival was monitored daily until 12 days post-inoculation. A log-rank test was performed to compare survival curves of JEV-inoculated ECEs. †, Significant difference between the survival curves of ECEs infected with the NS1′-expressing viruses (S982-A67G-IC and JaTH-IC) and JaTH-G66A-IC (P<0.05); ‡, significant difference between the survival curves of ECEs infected with the NS1′-expressing viruses and S982-IC (P<0.05); **, significant difference between the survival curves of ECEs infected with the NS1′-expressing viruses and the NS1′-non-expressing viruses (JaTH-G67A-IC and JaTH-G66A-IC) (P<0.01). (c, d) On day 5 post-inoculation, virus titres were determined from homogenized tissues of live (n=3–4) and dead (n=6–10) ECEs that had been inoculated with 10^4 p.f.u. per egg of the indicated viruses. The distribution of the virus titres from embryonic tissue samples (c) and from the yolk sac (d) was plotted. The values between two groups were tested by one-way ANOVA. Asterisks indicate statistical significance (*P<0.05; **P<0.01) in the difference of titres between the NS1′-expressing viruses and the NS1′-non-expressing viruses. Underlining indicates the NS1′-expressing viruses.

CO_2. The supernatants were harvested at 0, 24, 48 and 72 h p.i. and stored in aliquots at −80 °C prior to titration.

Focus formation and virus titration. Focus formation was performed on BHK and DF-1 cells as described previously (Espada-Murao & Morita, 2011). Virus titres were determined by plaque-forming assays on BHK cells and expressed as p.f.u. ml^{-1}. A 10-fold serial dilution of viral stocks was used for infection, and an overlay of MEM with 2 % FCS and 1 % methylcellulose was added after viral adsorption. Cells were incubated at 37 °C with 5 % CO_2 for 4 days, fixed with 4 % paraformaldehyde in phosphate buffer (WAKO) and stained with 0.1 % crystal violet in 10 % ethanol (Hayasaka *et al.*, 2009).

NS1′ antibody. NS1′ polyclonal antibodies were produced from C57BL/6j mice (Japan SLC Co.), which were injected with a peptide antigen (Fig. S5). The antigen was prepared following a procedure described previously (Yu *et al.*, 2007b). Here, the *NS1′* gene was amplified using primers 5′-AAAGGATCCTCAGCTGGGCCTTC-TGG-3′and 5′-AAACTCGAGTCAGTGTAAGTGATGCC-3′, with the underlined nucleotides indicating restriction sites. PCR-amplified DNA fragment was digested with *Bam*HI and *Xho*I and cloned into the corresponding restriction sites of pGEX6p1 (GE Healthcare). The plasmids were transformed into BL21 Codon Plus (Agilent). Transformed *Escherichia coli* cells were cultured in 500 ml Terrific Broth containing ampicillin at a concentration of 50 μg ml^{-1}. Production of the NS1′ protein was induced by the addition of 0.5 mM IPTG when the OD_{600} of the culture reached 0.5. After IPTG induction at 37 °C for 3 h, the cells were harvested by centrifugation and washed with PBS. The cell suspension was sonicated in 5 s pulses at 10 s intervals for 5 min and centrifuged at 20 000 *g* for 35 min.

Supernatants were collected and filtered through 0.45 μM filter (Millipore) and applied to a glutathione–Sepharose 4B column (GE Healthcare). After washing with PBS twice, the purified protein was eluted with 50 mM Tris/HCl (pH 8.0), 100 mM NaCl, 10 mM glutathione. Protein concentrations were determined by the Bradford method and purity was confirmed by SDS-PAGE as described previously (Yu *et al.*, 2005). Purified proteins were aliquotted and stored at −30 °C prior to injection. Mouse anti-NS1 and rabbit anti-NS5 polyclonal antibodies were prepared applying a procedure similar to that of the anti-NS1′ antibody production (Yu *et al.*, 2007a). The experimental protocols were approved by the Animal Care and Use Committee, Nagasaki University, Japan.

Confocal laser-scanning microscopy. JEV infection was performed on a monolayer of cells on eight-well chamber slides (Nunc) at an m.o.i. of 10. At 48 h p.i., the cells were subjected to immunostaining as described previously (Espada-Murao & Morita, 2011). Briefly, the cells were fixed with 2 % paraformaldehyde, permeabilized with 1 % NP-40, blocked and stained. The primary antibodies used were as follows: mouse anti-NS1, mouse anti-NS1′ and rabbit anti-NS5 polyclonal antibodies. Alexa Fluor 488-conjugated anti-rabbit and Alexa Fluor 568-conjugated anti-mouse antibodies (Invitrogen) were used for secondary labelling. Finally, the cells were incubated with DAPI for nuclear counterstaining. Images were captured using an LSM780 confocal laser-scanning microscope (Carl Zeiss).

Western blotting. JEV infection was performed on a monolayer of cells on 12-well plates at an m.o.i. of 10. At 48 h p.i., the cells were washed with PBS and resuspended in 100 μl lysis buffer [8 M urea, 500 mM Tris/HCl (pH 8.0), 2.5 mM EDTA]. After 30 min on ice, the cells were centrifuged at 20 000 ***g*** for 30 min at 4 °C. Each supernatant was mixed with acetone at a volume 10 times that of the supernatant and kept at −80 °C. The chilled samples were centrifuged under the same conditions as above and each supernatant was discarded. The pellets were mixed with SDS-PAGE sample buffer [62.5 mM Tris/HCl (pH 6.8), 4 % SDS, 10 % 2-mercaptoethanol, 0.1 % bromophenol blue] and then heated at 95 °C for 3 min. Equal volumes of samples were loaded onto a 10–20 % polyacrylamide gradient gel (e-PAGEL; ATTO) and separated by SDS-PAGE. Western blotting was performed as described previously (Okamoto *et al.*, 2012; Yu *et al.*, 2007a). For the primary antibody reaction, PVDF membranes (Millipore) were treated with mouse anti-β-actin (Santa Cruz Biotechnology, 1 : 1000 dilution), mouse anti-NS1 (1 : 250 dilution), mouse anti-NS1′ (1 : 250 dilution) or rabbit anti-NS5 (1 : 250 dilution) polyclonal antibodies. For the secondary antibody reaction, membranes were treated with the corresponding anti-mouse IgG–HRP (Santa Cruz Biotechnology, 1 : 10 000 dilution) or anti-rabbit IgG–HRP (Santa Cruz Biotechnology, 1 : 10 000 dilution). Protein bands were developed using Luminata Forte Western HRP Substrate (Millipore) and detected by using an LAS-4000 Mini Luminescent Image Analyzer (Fujifilm). The intensity of bands was calculated using ImageJ software (Schneider *et al.*, 2012).

Co-IP. The co-IP procedure was performed using protein A/G–Sepharose (GE Healthcare) with purified anti-NS1 or anti-NS5 polyclonal antibodies. JEV infection was performed on a monolayer of BHK and DF-1 cells in 150 cm^2 flasks. PBS was used in the control cells. At 48 h p.i., the cells were washed with cold PBS and lysed with 50 mM Tris/HCl (pH 7.5), 150 mM NaCl, 1 mM EDTA, 1 % NP-40 and protease inhibitor (Thermo Scientific). The lysed solutions were sonicated for 15–30 s and centrifuged at 12 000 ***g*** for 10 min. Supernatants were collected and subjected to co-IP according to the manufacturer's instructions. Briefly, after the antigen–antibody reaction had taken place at 4 °C for 1 h, protein A/G–Sepharose was added. After incubation at 4 °C overnight, the solutions were centrifuged at 12 000 ***g*** for 20 s and the pellets washed three times with wash buffer [50 mM Tris/HCl (pH 7.5), 50 mM NaCl, 1 mM EDTA, protease inhibitor]. Finally, elution was achieved through the use of SDS-PAGE sample buffer. Western blotting was carried out following the procedure above.

Real-time quantitative RT-PCR. JEV infection was performed on a monolayer of cells on 24-well plates at an m.o.i. of 0.1. At the indicated times, total RNA was harvested from cells using an RNeasy Mini kit (Qiagen). One microgram of RNA in a total volume of 20 μl was reverse transcribed with a Prime Script RT Reagent kit (TaKaRa) to obtain cellular mRNA and JEV RNA. Two microlitres of the product was used for real-time PCR (Applied Biosystems) with SYBR Premix Ex *Taq* II (TaKaRa). The number of copies of viral RNA, β-actin and glyceraldehyde 3-phosphate dehydrogenase (GAPDH) mRNAs was calculated by absolute quantification based on *in vitro*-transcribed JEV RNA, β-actin and GAPDH standards (Li *et al.*, 2013). The real-time RT-PCR primers are shown in Table S3.

Inoculation of ECEs. ECEs have been used for virus isolation and propagation (Clavijo *et al.*, 2000; Crespo *et al.*, 2009). Infection of ECEs with JEV in the present study was performed following the basic procedure used for WNV (Osorio *et al.*, 2012) and Crimean–Congo haemorrhagic fever virus (Xia *et al.*, 2013). Seven-day old ECEs were assigned per experimental or control group. These ECEs were inoculated with 200 μl viral inoculum (10^4 or 10^2 p.f.u. for experimental groups) or PBS (for control group) into the allantoic cavity, after which they were kept at 37 °C in an incubator. ECEs were candled once daily after inoculation to check their survival until 12 days post-inoculation. Dead ECEs in the first 24 h post-inoculation were discarded and the cause of their death was considered to be non-specific (Xia *et al.*, 2013).

Virus recovery from tissues and titration. Both dead and live ECEs at day 5 post-inoculation were chilled at 4 °C for 1 h in preparation for collecting tissues. The egg surface was disinfected with 70 % ethanol. The portion of the egg shell that covered the air cell was disinfected and a pair of sterile forceps was used to crack and remove the egg shell over the air cell. Embryonic tissues and yolk sac tissues were grasped with sterile forceps and stored in cryovials at −80 °C prior to titration. These samples were homogenized on a 70 μm cell strainer (BD Biosciences) with a particular volume (mg μl^{-1}) of medium. The virus titre in each sample was determined by a plaque-forming assay in BHK cells and expressed as p.f.u. (g tissue)$^{-1}$ (Hayasaka *et al.*, 2009).

ACKNOWLEDGEMENTS

We thank Dr Ichiro Kurane and Dr Tomohiko Takasaki from the National Institute of Infectious Diseases, Tokyo, Japan, for providing strain JaTH160; Dr Jiro Yasuda from the Department of Emerging Infectious Diseases, Institute of Tropical Medicine (NEKKEN), Nagasaki University, Nagasaki, Japan, for providing technical advice; and Mr Kotaro Aoki from the Department of Virology, Institute of Tropical Medicine (NEKKEN), Nagasaki University, Nagasaki, Japan, for providing technical assistance. This study was supported by a Grant-in-Aid for Scientific Research from the Ministry of Education, Culture, Sports, Science and Technology (MEXT), Japan, Young Researcher Overseas Visits Program for Vitalizing Brain Circulation, MEXT, Japan, the Global COE program, MEXT, Japan, the Japan Initiative for Global Network on Infectious Diseases (J-GRID), MEXT, Japan, and a Grant-in-Aid for Scientific Research from the Ministry of Health, Labour, and Welfare, Japan.

REFERENCES

Avirutnan, P., Fuchs, A., Hauhart, R. E., Somnuke, P., Youn, S., Diamond, M. S. & Atkinson, J. P. (2010). Antagonism of the

complement component C4 by flavivirus nonstructural protein NS1. *J Exp Med* **207**, 793–806.

Blitvich, B. J., MacKenzie, J. S., Coelen, R. J., Howard, M. J. & Hall, R. A. (1995). A novel complex formed between the flavivirus E and NS1 proteins: analysis of its structure and function. *Arch Virol* **140**, 145–156.

Brierley, I., Pennell, S. & Gilbert, R. J. (2007). Viral RNA pseudoknots: versatile motifs in gene expression and replication. *Nat Rev Microbiol* 5, 598–610.

Chen, L. K., Liao, C. L., Lin, C. G., Lai, S. C., Liu, C. I., Ma, S. H., Huang, Y. Y. & Lin, Y. L. (1996). Persistence of Japanese encephalitis virus is associated with abnormal expression of the nonstructural protein NS1 in host cells. *Virology* **217**, 220–229.

Chung, K. M., Liszewski, M. K., Nybakken, G., Davis, A. E., Townsend, R. R., Fremont, D. H., Atkinson, J. P. & Diamond, M. S. (2006a). West Nile virus nonstructural protein NS1 inhibits complement activation by binding the regulatory protein factor H. *Proc Natl Acad Sci U S A* **103**, 19111–19116.

Chung, K. M., Nybakken, G. E., Thompson, B. S., Engle, M. J., Marri, A., Fremont, D. H. & Diamond, M. S. (2006b). Antibodies against West Nile virus nonstructural protein NS1 prevent lethal infection through Fc γ receptor-dependent and -independent mechanisms. *J Virol* **80**, 1340–1351.

Chung, K. M., Thompson, B. S., Fremont, D. H. & Diamond, M. S. (2007). Antibody recognition of cell surface-associated NS1 triggers Fc-γ receptor-mediated phagocytosis and clearance of West Nile virus-infected cells. *J Virol* **81**, 9551–9555.

Clavijo, A., Heckert, R. A., Dulac, G. C. & Afshar, A. (2000). Isolation and identification of bluetongue virus. *J Virol Methods* **87**, 13–23.

Crespo, R., Shivaprasad, H. L., França, M. & Woolcock, P. R. (2009). Isolation and distribution of West Nile virus in embryonated chicken eggs. *Avian Dis* **53**, 608–612.

Espada-Murao, L. A. & Morita, K. (2011). Delayed cytosolic exposure of Japanese encephalitis virus double-stranded RNA impedes interferon activation and enhances viral dissemination in porcine cells. *J Virol* **85**, 6736–6749.

Ferreira, V. P., Pangburn, M. K. & Cortés, C. (2010). Complement control protein factor H: the good, the bad, and the inadequate. *Mol Immunol* **47**, 2187–2197.

Firth, A. E. & Atkins, J. F. (2009). A conserved predicted pseudoknot in the NS2A-encoding sequence of West Nile and Japanese encephalitis flaviviruses suggests NS1′ may derive from ribosomal frameshifting. *Virol J* **6**, 14.

Fujii, Y., Kitaura, K., Nakamichi, K., Takasaki, T., Suzuki, R. & Kurane, I. (2008). Accumulation of T-cells with selected T-cell receptors in the brains of Japanese encephalitis virus-infected mice. *Jpn J Infect Dis* **61**, 40–48.

Ghosh, D. & Basu, A. (2009). Japanese encephalitis – a pathological and clinical perspective. *PLoS Negl Trop Dis* **3**, e437.

Hayasaka, D., Gritsun, T. S., Yoshii, K., Ueki, T., Goto, A., Mizutani, T., Kariwa, H., Iwasaki, T., Gould, E. A. & Takashima, I. (2004). Amino acid changes responsible for attenuation of virus neurovirulence in an infectious cDNA clone of the Oshima strain of tick-borne encephalitis virus. *J Gen Virol* **85**, 1007–1018.

Hayasaka, D., Nagata, N., Fujii, Y., Hasegawa, H., Sata, T., Suzuki, R., Gould, E. A., Takashima, I. & Koike, S. (2009). Mortality following peripheral infection with tick-borne encephalitis virus results from a combination of central nervous system pathology, systemic inflammatory and stress responses. *Virology* **390**, 139–150.

Khromykh, A. A., Sedlak, P. L., Guyatt, K. J., Hall, R. A. & Westaway, E. G. (1999). Efficient trans-complementation of the flavivirus kunjin NS5 protein but not of the NS1 protein requires its coexpression with other components of the viral replicase. *J Virol* **73**, 10272–10280.

Le Flohic, G., Porphyre, V., Barbazan, P. & Gonzalez, J. P. (2013). Review of climate, landscape, and viral genetics as drivers of the Japanese encephalitis virus ecology. *PLoS Negl Trop Dis* **7**, e2208.

Li, Z., Wang, Y., Li, X., Li, X., Cao, H. & Zheng, S. J. (2013). Critical roles of glucocorticoid-induced leucine zipper in infectious bursal disease virus (IBDV)-induced suppression of type I Interferon expression and enhancement of IBDV growth in host cells via interaction with VP4. *J Virol* **87**, 1221–1231.

Lin, Y. L., Chen, L. K., Liao, C. L., Yeh, C. T., Ma, S. H., Chen, J. L., Huang, Y. L., Chen, S. S. & Chiang, H. Y. (1998). DNA immunization with Japanese encephalitis virus nonstructural protein NS1 elicits protective immunity in mice. *J Virol* **72**, 191–200.

Lindenbach, B. D. & Rice, C. M. (1997). *trans*-Complementation of yellow fever virus NS1 reveals a role in early RNA replication. *J Virol* **71**, 9608–9617.

Lindenbach, B. D. & Rice, C. M. (1999). Genetic interaction of flavivirus nonstructural proteins NS1 and NS4A as a determinant of replicase function. *J Virol* **73**, 4611–4621.

MacKenzie, J. M., Jones, M. K. & Young, P. R. (1996). Immunolocalization of the dengue virus nonstructural glycoprotein NS1 suggests a role in viral RNA replication. *Virology* **220**, 232–240.

Mason, P. W. (1989). Maturation of Japanese encephalitis virus glycoproteins produced by infected mammalian and mosquito cells. *Virology* **169**, 354–364.

Matsufuji, S., Matsufuji, T., Wills, N. M., Gesteland, R. F. & Atkins, J. F. (1996). Reading two bases twice: mammalian antizyme frameshifting in yeast. *EMBO J* **15**, 1360–1370.

Melian, E. B., Hinzman, E., Nagasaki, T., Firth, A. E., Wills, N. M., Nouwens, A. S., Blitvich, B. J., Leung, J., Funk, A. & other authors (2010). NS1′ of flaviviruses in the Japanese encephalitis virus serogroup is a product of ribosomal frameshifting and plays a role in viral neuroinvasiveness. *J Virol* **84**, 1641–1647.

Morita, K., Tadano, M., Nakaji, S., Kosai, K., Mathenge, E. G., Pandey, B. D., Hasebe, F., Inoue, S. & Igarashi, A. (2001). Locus of a virus neutralization epitope on the Japanese encephalitis virus envelope protein determined by use of long PCR-based region-specific random mutagenesis. *Virology* **287**, 417–426.

Muylaert, I. R., Chambers, T. J., Galler, R. & Rice, C. M. (1996). Mutagenesis of the N-linked glycosylation sites of the yellow fever virus NS1 protein: effects on virus replication and mouse neurovirulence. *Virology* **222**, 159–168.

Okamoto, K., Kinoshita, H., Parquet, M. C., Raekiansyah, M., Kimura, D., Yui, K., Islam, M. A., Hasebe, F. & Morita, K. (2012). Dengue virus strain DEN2 16681 utilizes a specific glycochain of syndecan-2 proteoglycan as a receptor. *J Gen Virol* **93**, 761–770.

Osorio, J. E., Ciuoderis, K. A., Lopera, J. G., Piedrahita, L. D., Murphy, D., Levasseur, J., Carrillo, L., Ocampo, M. C. & Hofmeister, E. (2012). Characterization of West Nile viruses isolated from captive American Flamingoes (*Phoenicopterus ruber*) in Medellin, Colombia. *Am J Trop Med Hyg* **87**, 565–572.

Plant, E. P. & Dinman, J. D. (2006). Comparative study of the effects of heptameric slippery site composition on −1 frameshifting among different eukaryotic systems. *RNA* **12**, 666–673.

Schlesinger, J. J. (2006). Flavivirus nonstructural protein NS1: complementary surprises. *Proc Natl Acad Sci U S A* **103**, 18879–18880.

Schneider, C. A., Rasband, W. S. & Eliceiri, K. W. (2012). NIH Image to ImageJ: 25 years of image analysis. *Nat Methods* **9**, 671–675.

Solomon, T. (2004). Flavivirus encephalitis. *N Engl J Med* **351**, 370–378.

Sumiyoshi, H., Mori, C., Fuke, I., Morita, K., Kuhara, S., Kondou, J., Kikuchi, Y., Nagamatu, H. & Igarashi, A. (1987). Complete nucleotide

sequence of the Japanese encephalitis virus genome RNA. *Virology* **161**, 497–510.

Sumiyoshi, H., Hoke, C. H. & Trent, D. W. (1992). Infectious Japanese encephalitis virus RNA can be synthesized from in vitro-ligated cDNA templates. *J Virol* **66**, 5425–5431.

van den Hurk, A. F., Ritchie, S. A. & MacKenzie, J. S. (2009). Ecology and geographical expansion of Japanese encephalitis virus. *Annu Rev Entomol* **54**, 17–35.

Westaway, E. G., Brinton, M. A., Gaidamovich, S. Ya, Horzinek, M. C., Igarashi, A., Kääriäinen, L., Lvov, D. K., Porterfield, J. S., Russell, P. K. & Trent, D. W. (1985). *Flaviviridae. Intervirology* **24**, 183–192.

Wilson, J. R., de Sessions, P. F., Leon, M. A. & Scholle, F. (2008). West Nile virus nonstructural protein 1 inhibits TLR3 signal transduction. *J Virol* **82**, 8262–8271.

Winkelmann, E. R., Widman, D. G., Suzuki, R. & Mason, P. W. (2011). Analyses of mutations selected by passaging a chimeric flavivirus identify mutations that alter infectivity and reveal an interaction between the structural proteins and the nonstructural glycoprotein NS1. *Virology* **421**, 96–104.

Xia, H., Zhao, J., Li, Y., Yin, S., Tang, S., Zhang, Z., Yu, J., Kou, Z., Fan, Z. & Li, T. (2013). Infection and propagation of Crimean-Congo hemorrhagic fever virus in embryonated chicken eggs. *Virus Res* **173**, 344–349.

Ye, Q., Li, X. F., Zhao, H., Li, S. H., Deng, Y. Q., Cao, R. Y., Song, K. Y., Wang, H. J., Hua, R. H. & other authors (2012). A single nucleotide mutation in NS2A of Japanese encephalitis-live vaccine virus (SA14-14-2) ablates NS1′ formation and contributes to attenuation. *J Gen Virol* **93**, 1959–1964.

Youn, S., Li, T., McCune, B. T., Edeling, M. A., Fremont, D. H., Cristea, I. M. & Diamond, M. S. (2012). Evidence for a genetic and physical interaction between nonstructural proteins NS1 and NS4B that modulates replication of West Nile virus. *J Virol* **86**, 7360–7371.

Young, L. B., Melian, E. B. & Khromykh, A. A. (2013). NS1′ colocalizes with NS1 and can substitute for NS1 in West Nile virus replication. *J Virol* **87**, 9384–9390.

Yu, F., Le, M. Q., Inoue, S., Thai, H. T., Hasebe, F., Del Carmen Parquet, M. & Morita, K. (2005). Evaluation of inapparent nosocomial severe acute respiratory syndrome coronavirus infection in Vietnam by use of highly specific recombinant truncated nucleocapsid protein-based enzyme-linked immunosorbent assay. *Clin Diagn Lab Immunol* **12**, 848–854.

Yu, F., Hasebe, F., Inoue, S., Mathenge, E. G. & Morita, K. (2007a). Identification and characterization of RNA-dependent RNA polymerase activity in recombinant Japanese encephalitis virus NS5 protein. *Arch Virol* **152**, 1859–1869.

Yu, F., Le, M. Q., Inoue, S., Hasebe, F., Parquet, M. C., Morikawa, S. & Morita, K. (2007b). Recombinant truncated nucleocapsid protein as antigen in a novel immunoglobulin M capture enzyme-linked immunosorbent assay for diagnosis of severe acute respiratory syndrome coronavirus infection. *Clin Vaccine Immunol* **14**, 146–149.

Original paper
Title page

Title
Pathologic potential of variant clones of the Oshima strain of Far-Eastern subtype tick-borne encephalitis virus

Short title
Variant clones of FE-TBEV

Authors
Le Xuan Luat, Mya Myat Ngwe Tun, Corazon C. Buerano, Kotaro Aoki, Kouichi Morita and Daisuke Hayasaka

Affiliation
Department of Virology, Institute of Tropical Medicine, GCOE program, Leading Graduate School Program, Nagasaki University, Nagasaki, Nagasaki, Japan

Corresponding Author
Daisuke Hayasaka, Department of Virology, Institute of Tropical Medicine, Nagasaki University, 1-12-4 Sakamoto, Nagasaki, 852-8523. E-mail address: hayasaka@nagasaki-u.ac.jp, Phone number: +81-95-819-7829, Fax number: +81-95-819-7830,

Number of figures: 4
Number of table: 1

Abstract

Tick-borne encephalitis virus (TBEV) is a zoonotic agent that causes acute central nervous system (CNS) disease in humans. We previously suggested that immune response in addition to CNS infection contribute to mouse mortality following TBEV infection. However, we did not examine the influence of virus variants in the previous study. Therefore, in this study, we investigated the biological and pathologic potentials of the variant clones in the TBEV Oshima strain. We isolated eight variant clones from the stock virus of the Oshima 5-10. These variants exhibited different plaque morphologies in BHK cells and pathogenic potentials in mice. Full sequences of viral genomes revealed that each of the variant clones except one had specific combinations of nucleotide and amino acid changes at certain positions different from the parent strain. We also showed that an amino acid substitution of Glu_{122}→Gly in the E protein could have affected virus infection and replication *in vivo*, as well as the attenuated pathogenicity in mice. These data confirm the presence of virus variants or quasispecies from the parent strain. Further elucidation of the effect of each variant clone on immune responses such as the T-cell response is an important priority in the development of an effective vaccine and treatment

strategies for tick-borne encephalitis.

Keywords
Far-eastern subtype TBEV, variant clones, E protein

Introduction

Tick-borne encephalitis virus (TBEV) is a causative agent of acute central nervous system (CNS) disease in humans [1-2]. TBEV is a member of the family *Flaviviridae*, genus *Flavivirus*, whose genome encodes three structural proteins (C, prM and E) and five non-structural (NS) proteins (NS1, NS2, NS3, NS4 and NS5) [2-4].

TBEV is prevalent over a wide area of Europe and Asia, and is divided into three subtypes comprising the European (Eu-), Siberian and Far Eastern (FE-) subtypes [5-6]. It has been suggested that the FE-TBEV is associated with a disease more severe than the one caused by the other subtypes [2]. TBEV can cause tick-borne encephalitis (TBE) which is a potentially fatal neurological infection affecting humans [4]. The virus can infect humans through the bite of an infected tick. The TBEV endemic areas of Europe and Asia correspond to the geographical distribution of *Ixodes* tick species [1, 7-11].

In human cases, the neurological symptoms include fever, headache, meningitis, meningoencephalitis and meningoencephalomyelitis [1]. However, the clinical features are not unique to TBE, and laboratory diagnosis is required to distinguish it from other neurological disorders [3, 12-13]. Although clinical symptoms vary from febrile illness to meningitis and encephalitis, the mechanism of severe encephalitis has not been fully elucidated.

The laboratory mouse model is commonly employed to elucidate the mechanism of disease development following TBEV infection *in vivo*. [14-17]. Recent works have proposed that CNS pathology following TBEV infection is a consequence of viral infection of the corresponding cells and the resulting inflammatory response [18].

Using a mouse model of infection with the Oshima strain of FE-TBEV, we have shown that immune and stress responses in addition to CNS infection contribute to mouse mortality [19-20]. These results indicated that the host immune response is likely to be a determinant of clinical outcome in this model [19-22]. However, we did not examine the influence of virus variants (quasi-species) in the mouse model experiments regarding TBEV Oshima infection.

Variants of TBEV may induce different degrees of pathology. Previous papers have reported that the amino acid mutations in the E protein of this virus exert an effect on its virulence and neuroinvasiveness [23-25]. For example, Mandl et al. reported that the E protein of the Neudoerfl strain of Eu-TBEV had several different mutations such as Glu_{122}→Gly, Ser_{158}→Arg, Gly_{159}→Arg and Glu_{201}→Lys after several passages in cultured cells. These mutations affected the binding sites of the protein and resulted in the attenuation of the virus *in vivo* [26]. It was also shown that neurovirulence of the Oshima strain of FE-TBEV was attenuated by the mutation at position 1579 (A→G, Asp_{483}→Gly) [23]. Thus, in this study, our purpose was to investigate the pathologic potential of the variants or quasispecies of the Oshima strain of FE-TBEV in a mouse model.

Methods

Virus and cell

Stock virus of the Oshima 5-10 strain of TBEV was prepared from infected cell culture medium of baby hamster kidney (BHK) [19]. The BHK cells were grown in

Eagle's Minimal Essential Medium (EMEM; Nissui Pharmaceutical Co.) containing 10% fetal calf serum (FCS). All experiments using live TBEV were performed in a biosafety level 3 laboratory at the Institute of Tropical Medicine, Nagasaki University according to the standard Biosafety Level 3 guidelines.

Plaque assay

Virus titers were determined by plaque forming assays in BHK cells [19]. Briefly, monolayers of BHK cells were grown in 24-well plates and infected with serial dilutions of the virus in culture medium. After incubation at 37°C for 90 minutes, culture medium containing 1% methyl cellulose was added to each well. Cells were then incubated for four days, after which, the medium was removed and cells were stained with crystal violet. Viral titers were expressed as pfu/ ml of the diluted viruses in culture medium.

Cloning of Oshima 5-10 by limiting dilution

BHK cells were grown in four 96-well plates and then inoculated with Oshima 5-10 at a concentration of 0.1 pfu /well. Cytopathic effects (CPE) were observed in less than 10 wells per plate. The infected culture fluids in these wells were harvested and inoculated in fresh BHK cells, and the procedure of identifying CPE and inoculation in BHK cells was repeated. Finally, the stock viruses of each clone were prepared from cell culture medium of BHK.

Mice

C57BL/6j (B6) mice were purchased from Japan SLC Corporation. Five-week old female B6 mice were subcutaneously inoculated with 10^4 PFU of TBEV Oshima 5-10 parent (Oshima-pt) and Oshima clones diluted in 200 μl of EMEM containing 2% FCS. Mock-infected mice were inoculated with the supernatant medium of uninfected BHK cells. The mice were weighed daily and observed for clinical signs. The animal experiments were performed in accordance with the Fundamental Guidelines for Proper Conduct of Animal Experiments and Related Activities in Academic Research Institutions under the jurisdiction of the Ministry of Education, Culture, Sports, Science and Technology. The experimental protocols were approved by the Nagasaki University Animal Care and Use Committee (approval number: 091130-2-7 / 0912080807-7).

Virus titrations

At nine days post-infection (p.i.) with 10^4 PFU of TBEV Oshima clones, mouse brains and spleens were collected after perfusion with cold PBS. The spleens were immediately immersed in RNAlater (Ambion). The collected tissues were stored at -80°C until they were used.

The brains were homogenized in ten volumes of PBS containing 10% FCS and diluted with EMEM with 2% FCS. Virus titers were determined by plaque-forming assays in BHK cells and were expressed as pfu/g of tissue.

Total RNA was extracted from spleens using RNeasy Lipid Tissue Mini Kit (Qiagen) according to the manufacturer's instructions. The levels of viral RNA were measured by real time-PCR as demonstrated previously [27-28]. The copy numbers were calculated as a ratio of the copy numbers in 100 ng of RNA

Genome sequence of the Oshima 5-10 clones

Viral RNA of each Oshima 5-10 clone was extracted from the cell culture fluids of

each stock virus using QIAquick PCR Purification Kit (QIAGEN) according to the manufacturer's protocol. Reverse transcription was performed using Superscript III reverse transcriptase (Invitrogen) and random hexamers. PCR was performed to cover the whole genome sequence using TAKARA Ex *Taq* DNA polymerase (TAKARA BIO Inc.). The cycle sequencing reaction was performed using BigDye Terminator v3.1 Cycle Sequencing Kit (Life Technologies), and the DNA sequence was determined in the Applied Biosystems 3730 DNA Analyzer (Life Technologies).

Primers were designed based on the genome of Oshima 5-10 strain (GenBank Acc. No. AB062063.2). Sequence was performed in both directions with specific primer corresponding to each fragment. Sequence results were analyzed with MEGA5 [29] and Unipro Ugene [30]. The nucleotides sequences were aligned by ClustalX 2.1 [31] for full genome analyses.

3D structure of E protein of TBEV

The 3D structure of E protein was shown using the PyMOL Molecular Graphics System, Version 1.6 Schrödinger, LLC.

Results

Clones of the Oshima 5-10

We isolated and examined eight clones of Oshima 5-10 virus and designated them as Oshima-A4, A9, A11, B11, C1, E2, E3, and E7. The clones exhibited a different morphology of plaques in BHK cells (Fig. 1). Oshima-pt showed various sizes of plaques (Fig. 1). The plaque size of Oshima-A4, A9 and B11 was comparatively small, while that of C1 was large (Fig. 1). However, Oshima-A11, C1, E2, E3, and E7 virus caused a mixture of large and small plaques (Fig. 1). These results indicate that parent Oshima 5-10 virus consists of quasi-species based on the various sizes of plaques exhibited by the clones.

Pathogenicity of TBEV Oshima clones in mice

To examine the pathogenicity of TBEV Oshima clones in mice, we subcutaneously inoculated each clone in five corresponding B6 mice, which were then observed for morbidity (weight loss) and mortality. All Oshima-pt-infected mice exhibited weight loss and one mouse died at 12 days p.i. (Fig. 2). This observation was reproducible as in our previous study [19]. Oshima-A11, C1, E2 and E7 also caused weight loss in 4-5 mice and the death of 1-2 mice within 21 days p.i. similar to that of the parent virus (Fig. 2). Four Oshima-E3-infected mice exhibited weight loss and all mice survived (Fig. 2).

On the other hand, the small plaque-forming clones such as Oshima-A4, A9 and B11 did not cause any weight loss, clinical signs or death similar to the observations in the uninfected mice (Fig. 2).

These results indicate that only the clones producing small plaques, had attenuated virulence in mice and that the other Oshima clones with plaque-forming characteristics similar to those of the parent strain shared the same pathogenic potential as the parent strain.

Virus infections in brains and spleens of Oshima clones-infected mice

To observe the virus infection in the CNS, we investigated the infectious viral loads in the brains of Oshima clone-infected mice. Following inoculation with Oshima-pt, all mice exhibited more than 10^4 pfu/g of tissue in the brain (Fig. 3A). Oshima-A11-, C1-

and all E7-infected mice also showed more than 10^4 pfu/g of tissue in the brain (Fig. 3A). Following Oshima-E3 infection, one mouse showed a viral load in the brain, but the other two mice did not (Fig. 3A). The viral load in the brain of all Oshima-A4-, A9- and B11-infected mice was under the detection limit (Fig. 3A).

Next, we confirmed peripheral infections in Oshima clone-infected mice. We employed quantitative RT-PCR to detect viral RNA in the spleen instead of using plaque assay, because no infectious virus could be detected by this technique at nine days p.i. In all Oshima-pt-, A11-, C1-, E2- and E7-infected mice, viral RNA was detected, indicating that peripheral infection and replication occurred in these mice (Fig. 3B). In Oshima-E3-infected mice, one mouse showed peripheral infection, but no viral RNA was detected in the spleen of the other two mice (Fig. 3B). The viral RNA level was under the detection limit in two of three Oshima-A4- and B11- and in all of the A9-infected mice (Fig. 3B).

It is noteworthy that the Oshima-A4-, A9- and B11-infected mice with levels of viral RNA under the detection limit in the spleen did not exhibit viral infections in the brain either, indicating that viral infections did not occur or were very limited. These results suggest that Oshima-A4, A9 and B11 viruses exhibited very limited peripheral and CNS infection, and had an attenuated virulence in mice.

Genome sequence of Oshima 5-10 clones

We determined the full genome sequence of Oshima 5-10 clones by the direct sequence method. Each clone showed a few differences in nucleotide and amino acid at certain positions compared with Oshima-pt (Table 1). Interestingly, the Oshima-A4, A9 and B11 that showed small plaques and attenuated virulence had a common nucleotide substitution of A to G at position 1342 at the E-coding region, and it resulted in the substitution of amino acid from glutamic acid to glycine at position 122 of the E protein (Table 1). This substitution was not detected in Oshima-A11, C1, E2, E3 or E7 (Fig. 2). These results suggest that an amino acid change of glutamic acid to glycine in E protein affects the plaque morphology and may influence the biological activity of the Oshima strain of FE-TBEV.

Discussion

In this study, we examined eight variant clones from the stock virus of Oshima 5-10, a strain of FE-TBEV. These variants exhibited different pathogenic potentials in mice. Full sequences of viral genomes revealed that each of the variant clones except one had a specific combination of nucleotide and amino acid changes at certain positions different from the parent strain. These data confirm the presence of virus variants or quasispecies from the parent strain.

Oshima-A4, A9 and B11 exhibited attenuated virulence, whereas the others showed pathogenicity similar to that of the parent virus. None of the cloned variants in this study showed a significantly (log lank test) higher virulence than the parent virus, but in another study [14] Sofjin strain surpassed the parent strain in virulence. We also found that attenuated variants had a common amino acid substitution in E protein ($Glu_{122}\rightarrow Gly$). Mice inoculated with these variants exhibited no CNS viral entry and had very limited

peripheral infections. Using the Neudoerfl strain of Eu-TBEV, Mandl et al. reported that the same substitution of Glu_{122}→Gly in E protein appeared during adaptation in BHK-21 cells and that the amino acid substitution caused a reduction of virus virulence in mice. Thus, the Glu_{122}→Gly amino acid substitution could have affected virus infection and replication *in vivo* and the pathogenicity of both Eu-TBEV and FE-TBEV in mice.

The E protein of flaviviruses is classified as a class II virus membrane fusion protein and plays an important role in receptor binding and fusion of the virus membrane with the host cell membrane [32-34]. At neutral pH, E protein of mature flavivirus virion is a homodimer (Fig. 4A) and is located on the virus surface. Each monomer contains three different ß-barrel domains, namely domain I (DI), domain II (DII), and domain III (DIII) (Fig. 4A). DI is a structural domain, contains N-terminal and elongates with DII by a fusion loop (fp) at the tip of DII. This fp is buried through the interaction with a hydrophobic pocket between DI and DIII. DI connects to DIII by a single polypetide linker region. DIII is an immunoglobulin-like domain and connects to the C-terminal stem region and transmembrane (TM) domain [35-36]. At a low pH condition, the homodimer of E protein dissociates, and the fp is exposed and interacts with cell membrane [37]. At the next step, the monomer rearranges and associates into homotrimer (Fig. 4B), which then initiates hairpin formation. DIII and the stem region fold back towards the fusion loop as hemifusion [33]. Finally, the viral membrane completely fuses with the cell membrane through mixing of the outer membrane leaflet (viral membrane leaflet) and the inner membrane leaflet (cell membrane leaflet) and the opening of a fusion pore [38].

The substitution in E protein (Glu_{122}→Gly) is located in DII of E protein adjacent to the hinge region (Fig. 4A and 4B). During the membrane fusion process, the dissociation of homodimer and the consequent formation of homotrimer locates Glu_{122}→Gly on the surface of the homotrimer structure (Fig. 4B). DII of E protein contains fusion peptide that functions as an inert anchor or active center in the process of fusion between the viral envelope and cell membrane [39]. Mandl et al. showed that this substitution acquired potential HS-binding in this position and increased TBEV infectivity in BHK cells [26, 40]. They also showed that this substitution caused attenuation of virulence in mice, although the precise mechanism of the attenuation was not fully elucidated. In this study, we showed that Oshima-A4, A9 and B11 viruses exhibited small plaque size and attenuated virulence in mice. Attenuated virus replications of Oshima-A4, A9 and B11 might also be affected by HS binding [26] .

In this study, twelve nucleotide substitutions including the nucleotide that resulted in Glu_{122}→Gly were detected. It is noteworthy that Oshima-E3 exhibited attenuated virulence and one nucleotide change in E protein but that the change did not result in amino acid change. However, at this stage of our knowledge, it is difficult to explain how

these substitutions affect viral biology and virulence. Information on these substitutions has not been reported previously. Thus, investigations regarding the role of these nucleotide substitutions may provide important information in understanding the biology and pathogenesis of TBEV.

The laboratory mouse model has been commonly employed to study the pathology of encephalitic flaviviruses. Using the mouse model, we previously showed that the Oshima strain of FE-TBEV caused variation of fatal outcomes and we suggested that the immunopathogenetic process contributes to severe disease and mortality [19]. Furthermore, we showed that specific T-cell receptor (TCR) repertoires were present in dying mice during TBEV infection [41]. These data raise the possibility that there may be a variety of specific T-cell clones affecting either protective or pathogenetic functions in dying and recovering mice, indicating that the differentiation of specific T-cell clones is one of the key factors of the disease. However, the mechanism by which the differentiated T-cell clones appeared and developed remained unclear. Therefore, the variant amino acid of the variant clones found in this study might exert an effect on the various T-cell epitopes and on the differentiated T-cell clones in individual mice. Thus, the data from the present study could provide an important clue for understanding the variations of T cells affecting pathogenesis. Further investigations regarding the immunopathogenic T-cells is an important priority in the development of an effective vaccine and treatment strategies for TBE.

Acknowledgments

We thank Ikuo Takashima (Graduate School of Veterinary Medicine, Hokkaido University) for providing TBEV Oshima strain. This work was supported financially by KAKENHI [Grant-in-Aid for Challenging Exploratory Research (23658243)] from the Japan Society for the Promotion of Science, Health and Labour Sciences Research; Grant on Emerging and Re-emerging Infectious Diseases from the Japanese Ministry of Health, Labour and Welfare; the Global COE Program for Control of Emerging and Re-emerging Infectious Diseases (Nagasaki University); and the Japan Initiative for Global Research Network on Infectious Diseases.

References

1. Dumpis U, Crook D, Oksi J. Tick-borne encephalitis. Clin Infect Dis 1999; 28(4): 882-890.

2. Lindquist L, Vapalahti O. Tick-borne encephalitis. Lancet 2008; 371(9627): 1861-1871.

3. Mansfield KL, Johnson N, Phipps LP, Stephenson JR, Fooks AR, Solomon T. Tick-borne encephalitis virus - a review of an emerging zoonosis. The Journal of general virology 2009; 90(Pt 8): 1781-1794.
4. Gritsun TS, Lashkevich VA, Gould EA. Tick-borne encephalitis. Antiviral Research 2003; 57(1-2): 129-146.
5. Hayasaka D, Ivanov L, Leonova GN, Goto A, Yoshii K, Mizutani T, Kariwa H, Takashima I. Distribution and characterization of tick-borne encephalitis viruses from Siberia and far-eastern Asia. J Gen Virol 2001; 82(Pt 6): 1319-1328.
6. Ecker M, Allison SL, Meixner T, Heinz FX. Sequence analysis and genetic classification of tick-borne encephalitis viruses from Europe and Asia. J Gen Virol 1999; 80 (Pt 1): 179-185.
7. Burke SD, Monath PT. Flaviviruses. In: Knipe DM, Howley PM, Griffin DE, Lamb RA, Martin MA, Roizman B, Straus SE, eds. Fields virology. Philadelphia, PA: Lippincott Williams & Wilkins; 2001. pp. 991-1041.
8. Lundkvist k, Vene S, Golovljova I, Mavtchoutko V, Forsgren M, Kalnina V, Plyusnin A. Characterization of tick-borne encephalitis virus from Latvia: evidence for co-circulation of three distinct subtypes. Journal of medical virology 2001; 65(4): 730-735.
9. Skarpaas T GI, Vene S, Ljøstad U, Sjursen H, Plyusnin A, Lundkvist A. Tickborne encephalitis virus, Norway and Denmark. Emerg Infect Dis 2006; 12(6): 1136-1138.
10. Jääskeläinen AE TT, Uzcátegui NY, Alekseev AN, Vaheri A, Vapalahti O. Siberian subtype tickborne encephalitis virus, Finland. Emerg Infect Dis 2006; 12(10): 1568-1571.
11. Frey S, Mossbrugger I, Altantuul D, Battsetseg J, Davaadorj R, Tserennorov D, Buyanjargal T, Otgonbaatar D, Zoller L, Speck S, Wolfel R, Dobler G, Essbauer S. Isolation, preliminary characterization, and full-genome analyses of tick-borne encephalitis virus from Mongolia. Virus Genes 2012; 45(3): 413-425.
12. Charrel RN, Attoui H, Butenko AM, Clegg JC, Deubel V, Frolova TV, Gould EA, Gritsun TS, Heinz FX, Labuda M, Lashkevich VA, Loktev V, Lundkvist A, Lvov DV, Mandl CW, Niedrig M, Papa A, Petrov VS, Plyusnin A, Randolph S, Suss J, Zlobin VI, de Lamballerie X. Tick-borne virus diseases of human interest in Europe. Clinical microbiology and infection : the official publication of the European Society of Clinical Microbiology and Infectious Diseases 2004; 10(12): 1040-1055.
13. Holzmann H. Diagnosis of tick-borne encephalitis. Vaccine 2003; 21 Suppl 1: S36-40.
14. Chiba N, Iwasaki T, Mizutani T, Kariwa H, Kurata T, Takashima I. Pathogenicity of tick-borne encephalitis virus isolated in Hokkaido, Japan in mouse model. Vaccine 1999; 17(7-8): 779-787.
15. Pogodina VV, Savinov AP. Variation in the pathogenicity of viruses of the Tick-borne encephalitis complex for different animal species. I. experimental infection of mice and

hamsters. Acta Virol 1964; 8: 424-434.
16. Sokol F, Libikova H, Zemla J. Infectious ribonucleic acid from mouse brains infected with tick-borne encephalitis virus. Nature 1959; 184: 1581.
17. Vince V, Grcevic N. Development of morphological changes in experimental tick-borne meningoencephalitis induced in white mice by different virus doses. J Neurol Sci 1969; 9(1): 109-130.
18. Dorrbecker B, Dobler G, Spiegel M, Hufert FT. Tick-borne encephalitis virus and the immune response of the mammalian host. Travel Med Infect Dis 2010; 8(4): 213-222.
19. Hayasaka D, Nagata N, Fujii Y, Hasegawa H, Sata T, Suzuki R, Gould EA, Takashima I, Koike S. Mortality following peripheral infection with tick-borne encephalitis virus results from a combination of central nervous system pathology, systemic inflammatory and stress responses. Virology 2009; 390(1): 139-150.
20. Hayasaka D, Nagata N, Hasegawa H, Sata T, Takashima I, Koike S. Early mortality following intracerebral infection with the Oshima strain of tick-borne encephalitis virus in a mouse model. The Journal of veterinary medical science / the Japanese Society of Veterinary Science 2010; 72(4): 391-396.
21. Turtle L, Griffiths MJ, Solomon T. Encephalitis caused by flaviviruses. QJM 2012; 105(3): 219-223.
22. Hayasaka D. The Development of Encephalitis Following Tick-Borne Encephalitis Virus Infection in a Mouse Model. In: Ruzek D, ed. Daniel Ruzek. Croatia: Intech; 2011. pp. 9.
23. Goto A, Hayasaka D, Yoshii K, Mizutani T, Kariwa H, Takashima I. A BHK-21 cell culture-adapted tick-borne encephalitis virus mutant is attenuated for neuroinvasiveness. Vaccine 2003; 21(25-26): 4043-4051.
24. Mandl CW. Steps of the tick-borne encephalitis virus replication cycle that affect neuropathogenesis. Virus research 2005; 111(2): 161-174.
25. Rumyantsev AA, Murphy BR, Pletnev AG. A tick-borne Langat virus mutant that is temperature sensitive and host range restricted in neuroblastoma cells and lacks neuroinvasiveness for immunodeficient mice. Journal of virology 2006; 80(3): 1427-1439.
26. Mandl CW, Kroschewski H, Allison SL, Kofler R, Holzmann H, Meixner T, Heinz FX. Adaptation of tick-borne encephalitis virus to BHK-21 cells results in the formation of multiple heparan sulfate binding sites in the envelope protein and attenuation in vivo. Journal of virology 2001; 75(12): 5627-5637.
27. Fujii Y, Kitaura K, Nakamichi K, Takasaki T, Suzuki R, Kurane I. Accumulation of T-cells with selected T-cell receptors in the brains of Japanese encephalitis virus-infected mice. Jpn J Infect Dis 2008; 61(1): 40-48.
28. Hayasaka D, Aoki K, Morita K. Development of simple and rapid assay to detect

viral RNA of tick-borne encephalitis virus by reverse transcription-loop-mediated isothermal amplification. Virology journal 2013; 10: 68.

29. Tamura K, Peterson D, Peterson N, Stecher G, Nei M, Kumar S. MEGA5: molecular evolutionary genetics analysis using maximum likelihood, evolutionary distance, and maximum parsimony methods. Molecular biology and evolution 2011; 28(10): 2731-2739.

30. Okonechnikov K, Golosova O, Fursov M. Unipro UGENE: a unified bioinformatics toolkit. Bioinformatics 2012; 28(8): 1166-1167.

31. Chenna R, Sugawara H, Koike T, Lopez R, Gibson TJ, Higgins DG, Thompson JD. Multiple sequence alignment with the Clustal series of programs. Nucleic acids research 2003; 31(13): 3497-3500.

32. Stiasny K, Heinz FX. Flavivirus membrane fusion. J Gen Virol 2006; 87(Pt 10): 2755-2766.

33. Kielian M. Class II virus membrane fusion proteins. Virology 2006; 344(1): 38-47.

34. Rey Fa, Heinz FX, Mandl C, Kunz C, Harrison SC. The envelope glycoprotein from tick-borne encephalitis virus at 2 A resolution. Nature biotechnology 1995; 375(6529): 291-298.

35. Mukhopadhyay S, Kuhn RJ, Rossmann MG. A structural perspective of the flavivirus life cycle. Nat Rev Microbiol 2005; 3(1): 13-22.

36. Zhang Y, Zhang W, Ogata S, Clements D, Strauss JH, Baker TS, Kuhn RJ, Rossmann MG. Conformational changes of the flavivirus E glycoprotein. Structure 2004; 12(9): 1607-1618.

37. Stiasny K, Allison SL, Schalich J, Heinz FX. Membrane interactions of the tick-borne encephalitis virus fusion protein E at low pH. J Virol 2002; 76(8): 3784-3790.

38. Fritz R, Blazevic J, Taucher C, Pangerl K, Heinz FX, Stiasny K. The unique transmembrane hairpin of flavivirus fusion protein E is essential for membrane fusion. J Virol 2011; 85(9): 4377-4385.

39. Nieva JL, Agirre A. Are fusion peptides a good model to study viral cell fusion? Biochim Biophys Acta 2003; 1614(1): 104-115.

40. Kroschewski H, Allison SL, Heinz FX, Mandl CW. Role of heparan sulfate for attachment and entry of tick-borne encephalitis virus. Virology 2003; 308(1): 92-100.

41. Fujii Y, Hayasaka D, Kitaura K, Takasaki T, Suzuki R, Kurane I. T-cell clones expressing different T-cell receptors accumulate in the brains of dying and surviving mice after peripheral infection with far eastern strain of tick-borne encephalitis virus. Viral Immunol 2011; 24(4): 291-302.

Figure legends